HEALTH AND MEDICINE

Charge-switchable polymeric complex for glucose-responsive insulin delivery in mice and pigs

Jinqiang Wang[1,2,3]*, Jicheng Yu[3]*, Yuqi Zhang[3], Xudong Zhang[1,2], Anna R. Kahkoska[4], Guojun Chen[1,2], Zejun Wang[1,2], Wujin Sun[1,5], Lulu Cai[1,2,6], Zhaowei Chen[3], Chenggen Qian[7], Qundong Shen[7], Ali Khademhosseini[1,2,5,8,9], John B. Buse[4], Zhen Gu[1,2,3,5,10†]

Glucose-responsive insulin delivery systems with robust responsiveness that has been validated in animal models, especially in large animal models, remain elusive. Here, we exploit a new strategy to form a micro-sized complex between a charge-switchable polymer with a glucose-sensing moiety and insulin driven by electrostatic interaction. Both high insulin loading efficiency (95%) and loading capacity (49%) can be achieved. In the presence of a hyperglycemic state, the glucose-responsive phenylboronic acid (PBA) binds glucose instantly and converts the charge of the polymeric moiety from positive to negative, thereby enabling the release of insulin from the complex. Adjusting the ratio of the positively charged group to PBA achieves inhibited insulin release from the complex under normoglycemic conditions and promoted release under hyperglycemic conditions. Through chemically induced type 1 diabetic mouse and swine models, in vivo hyperglycemia-triggered insulin release with fast response is demonstrated after the complex is administrated by either subcutaneous injection or transdermal microneedle array patch.

INTRODUCTION

Diabetes mellitus and related secondary complications (*1*) affect and threaten the lives of 422 million people worldwide (*2*, *3*). Ideal diabetes management relies on the tight regulation of blood glucose levels (BGLs) to prevent long-term complications and optimize the quality of life. The conventional method for controlling BGLs involves the repeated subcutaneous injections of insulin based on glucose monitoring as well as expected carbohydrate intake and activity. Unfortunately, self-injection is fraught with challenges relating to adherence and dose selection, limiting the efficacy of glucose regulation and leading to a high risk of hypoglycemia, which can be fatal (*1*). Thus, various insulin delivery methods have been developed to address these problems and make insulin administration easier (*4*). Examples include insulin delivery systems that work in response to external stimuli like pH (*5*, *6*), temperature (*7*), ultrasonic radiation (*8*–*10*), mechanical force (*11*), ionic strength (*12*), magnetic field (*13*), and light (*14*). However, there remain challenges for these systems to quickly control the hyperglycemic state and reduce the risk of hypoglycemia upon insulin delivery.

To this end, substantial efforts have been devoted to the development of self-regulated, glucose-responsive insulin delivery systems (*15*, *16*). Most of these systems have relied on the specific interaction of glucose with glucose oxidase (GOx) (*17*–*21*), glucose-binding protein (*22*–*25*), and phenylboronic acid (PBA) (*26*–*34*). For example, GOx-catalyzed oxidation of glucose can generate acidic (*35*–*38*), hypoxic (*39*, *40*), and/or oxidative conditions (*40*–*42*), leading to the degradation, swelling, or dissolution of the matrices and subsequent release of preloaded insulin. Nevertheless, these systems still face several challenges, including slow response rate, low insulin loading efficiency, poor biocompatibility, and complicated manufacturing processes (*16*).

Here, we describe a new strategy for constructing a glucose-responsive insulin delivery formulation with fast response both in vitro and in vivo based on a glucose-triggered charge switch of a cationic polymer. As shown in Fig. 1A, a positively charged polymer is incorporated with pendant amino groups and PBA groups. In phosphate-buffered saline at pH 7.4 (PBS 7.4), this polymer is positively charged and is able to form a stable micro-sized suspension with a high insulin loading efficiency of 95% and a high loading capacity of 49% (Fig. 1B and fig. S1, A to D). In the presence of glucose, the binding of glucose to PBA in polymers leads to a decrease of positive charge density, thereby weakening the polymer's electrostatic attraction to insulin. Under hyperglycemic conditions, the positive charge of the polymer can be reversed, facilitating insulin release with fast response (Fig. 1, A and C). Meanwhile, this charge reversal is inhibited with the return to normoglycemia, thereby reducing the insulin release rate and subsequently reducing the risk of hypoglycemia.

RESULTS

Synthesis of polymers

A model polymer with pendant amino groups was synthesized through the free radical polymerization of tert-butyl (2-acrylamidoethyl) carbamate (Boc-EDAA) and the subsequent deprotection (scheme S1)

[1]Department of Bioengineering, University of California, Los Angeles, Los Angeles, CA, USA. [2]California NanoSystems Institute, University of California, Los Angeles, Los Angeles, CA, USA. [3]Joint Department of Biomedical Engineering, University of North Carolina at Chapel Hill and North Carolina State University, Raleigh, NC, USA. [4]Department of Medicine, University of North Carolina School of Medicine, Chapel Hill, NC 27599, USA. [5]Center for Minimally Invasive Therapeutics, University of California, Los Angeles, Los Angeles, CA, USA. [6]Personalized Drug Therapy Key Laboratory of Sichuan Province, Department of Pharmacy, Sichuan Provincial People's Hospital, University of Electronic, Science and Technology of China, Chengdu 611731, China. [7]Department of Polymer Science and Engineering and Key Laboratory of High-Performance Polymer Materials and Technology of MOE, School of Chemistry and Chemical Engineering, Nanjing University, Nanjing 210023, China. [8]Department of Chemical and Biomolecular Engineering, University of California, Los Angeles, Los Angeles, CA, USA. [9]Department of Radiology, University of California, Los Angeles, Los Angeles, CA, USA. [10]Jonsson Comprehensive Cancer Center, University of California, Los Angeles, Los Angeles, CA, USA.
*These authors contributed equally to this work.
†Corresponding author. Email: guzhen@ucla.edu

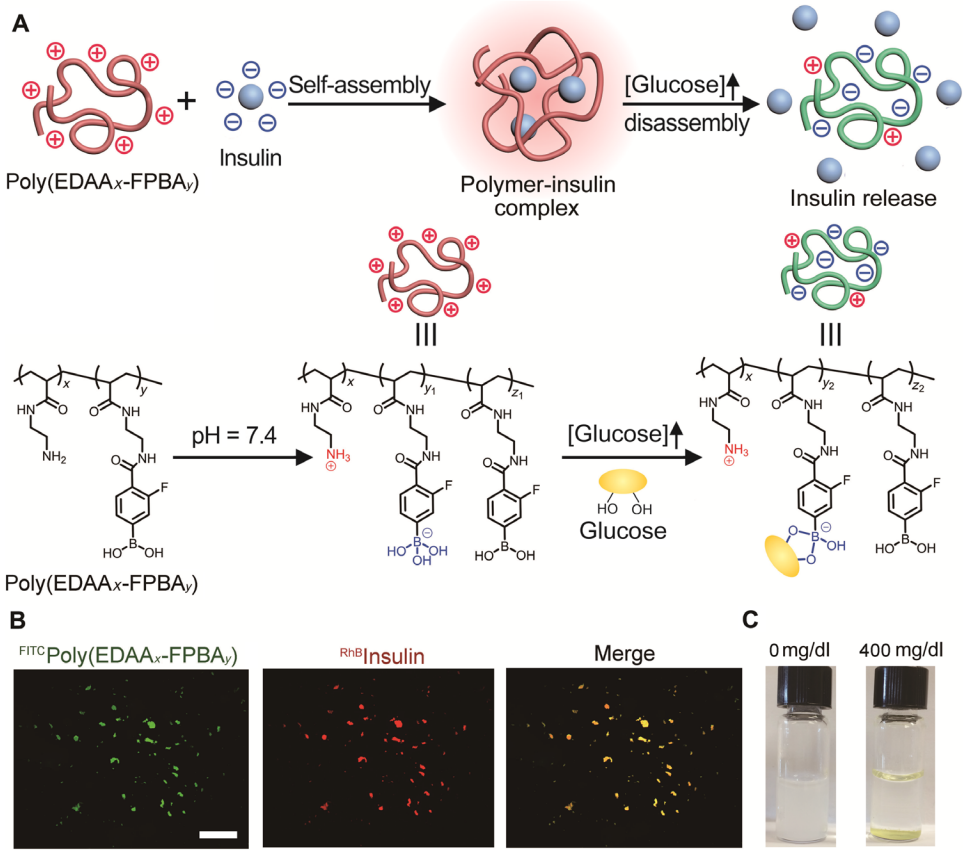

Fig. 1. Schematic of glucose-responsive charge-reversal polymers for insulin delivery. (**A**) Mechanism of glucose-sensitive charge reversal and enhanced insulin release from complex under a hyperglycemic state. The complex was prepared from a positively charged polymer and the negatively charged insulin via electrostatic interaction. (**B**) Representative fluorescence images of complex formed from poly(EDAA$_x$-FPBA$_y$) [green, fluorescein isothiocyanate (FITC)–labeled] and insulin (red, rhodamine B–labeled). Scale bar, 500 μm. (**C**) Representative images of the complex before (left) and after (right) treatment of glucose (400 mg/dl) for 3 hours at 37°C.

(*43*, *44*). The chemical structures were characterized by ^{1}H nuclear magnetic resonance (NMR) (fig. S2, A to C), while the molecular weight of poly(Boc-EDAA) was 8.7×10^3 g/mol with a polydispersity index of 2. 4-Carboxy-3-fluorophenylboronic acid (FPBA), with a suitable pK_a (where K_a is the acid dissociation constant) of 7.2 because of the introduction of fluorine (*34*), was activated as *N*-hydroxysuccinimide (NHS) ester and used to prepare poly(EDAA$_{0.4}$-FPBA$_{0.6}$) and poly(EDAA$_{0.7}$-FPBA$_{0.3}$) (fig. S2, D to F). As a comparison, 4-carboxyphenylboronic acid was also activated by NHS (*27*) (fig. S2G) and used to modify poly(EDAA) to produce poly(EDAA$_{0.4}$-PBA$_{0.6}$) (fig. S2H).

Preparation of insulin complex

Next, complexes were prepared from insulin and poly(EDAA$_{0.4}$-FPBA$_{0.6}$) with various ratios. Both insulin and poly(EDAA$_{0.4}$-FPBA$_{0.6}$) were dissolved in slightly acidic water and then mixed. After adjusting the pH to 7.4, a white suspension was obtained (Fig. 1C), indicating the formation of polymer-insulin complex. The complex precipitation was highly stable, suggesting a strong interaction between insulin and polymer. In addition, the water insolubility of poly(EDAA$_{0.4}$-FPBA$_{0.6}$) is proposed to be vital for stabilizing the complex formed between polymer and insulin (*45*).

In vitro glucose-responsive performance

The ability of polymers binding to glucose was evaluated in PBS 7.4 with varying clinically relevant glucose concentrations of 100, 200, and 400 mg/dl. Polymer-insulin complexes composed of an equal weight of insulin and polymer, namely, poly(EDAA$_{0.4}$-FPBA$_{0.6}$)–complexed insulin (designated as F-insulin), poly(EDAA$_{0.4}$-PBA$_{0.6}$)–complexed insulin (designated as B-insulin), and poly(EDAA)–complexed insulin (designated as N-insulin), were prepared. After the addition of glucose to F-insulin solution containing insulin [1 mg (or 28.8 U)/ml], the concentration of glucose decreased by around 10, 15, and 35 mg/dl for glucose solutions of 100, 200, and 400 mg/dl, respectively, within 10 min (Fig. 2A and fig. S1E). Unexpectedly, further binding of glucose to F-insulin was observed in glucose solution (400 mg/dl) such that a total decrease of 50 mg/dl of the glucose concentration within 2 hours was observed, indicating that approximately 90% of FPBA moiety was bound to glucose, probably ascribed to the enhanced diol-capturing ability arising from adjacent amino groups (*46*, *47*). As a comparison, no glucose binding or negligible binding was observed for the solution of B-insulin and N-insulin (Fig. 2, B and C) (*48*).

To determine whether glucose binding could lead to the reduction of positive charge density on polymers, polymeric nanoparticles were prepared by dripping the concentrated acidic aqueous solution of poly(EDAA$_{0.4}$-FPBA$_{0.6}$) or poly(EDAA$_{0.4}$-PBA$_{0.6}$) to PBS 7.4. Both polymers formed stable spherical nanoparticles as measured by the dynamic laser scattering (DLS) and transmission electron microscopy (TEM) (Fig. 2, D and E). Meanwhile, the original ζ potential of poly(EDAA$_{0.4}$-FPBA$_{0.6}$) nanoparticles was +40 mV in the absence of glucose (Fig. 2F), which gradually decreased to +22 mV

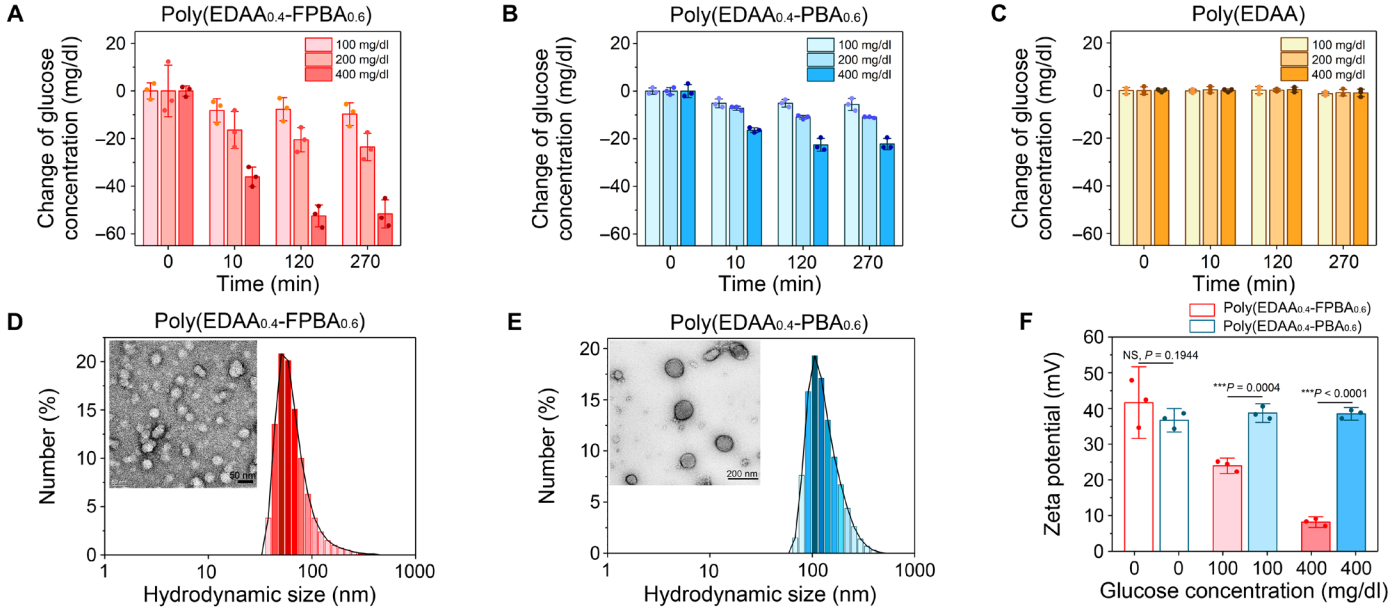

Fig. 2. The glucose binding and charge-switch study. (**A** to **C**) Glucose concentration–dependent glucose-binding ability of F-insulin (A), B-insulin (B), and N-insulin (C). The complexes were incubated in glucose solutions (100, 200, or 400 mg/dl). Data points are means ± SD ($n = 3$). (**D** and **E**) Hydrodynamic size distribution determined by DLS and representative TEM images of nanoparticles prepared from poly(EDAA$_{0.4}$-FPBA$_{0.6}$) (D) and poly(EDAA$_{0.4}$-PBA$_{0.6}$) (E). (**F**) Glucose concentration–dependent ζ potentials of nanoparticles prepared from poly(EDAA$_{0.4}$-FPBA$_{0.6}$) and poly(EDAA$_{0.4}$-PBA$_{0.6}$). Data points are means ± SD ($n = 3$). Statistical significance was calculated using Student's *t* test. ***$P < 0.001$. NS, not significant.

in glucose solution of 100 mg/dl and further decreased to +8 mV in glucose solution of 400 mg/dl. Because poly(EDAA$_{0.4}$-FPBA$_{0.6}$) precipitated within 5 min after the glucose concentration increased to 400 mg/dl, we were unable to measure the ζ potential of poly(EDAA$_{0.4}$-FPBA$_{0.6}$)–glucose complex directly. However, based on both the high efficiency of glucose binding (~90% FPBA bound to glucose) and the pK_a of FPBA (~6.4) in glucose solution (400 mg/dl) (*34*), about 90% of FPBA should carry a negative charge at pH 7.4, therefore making poly(EDAA$_{0.4}$-FPBA$_{0.6}$) negatively charged.

Next, the insulin release from the complexes upon glucose concentration variation was assessed. The insulin release kinetics can be tuned by varying the weight ratios of poly(EDAA$_{0.4}$-FPBA$_{0.6}$) to insulin (fig. S3, A to C), with F-insulin showing the most robust insulin release kinetics, which was further validated by measuring the fluorescence intensity of rhodamine B–labeled insulin (RhB-insulin) released from F-insulin (Fig. 3A and fig. S1F). In contrast, B-insulin or poly(EDAA$_{0.7}$-FPBA$_{0.3}$)–insulin complex exhibited a relatively slow insulin release rate (Fig. 3B and fig. S3D). Moreover, the insulin release rate was steadily increased in response to glucose concentration variation (from 100 to 400 mg/dl), achieving a maximum of fourfold enhancement (Fig. 3C). This fast insulin release kinetics upon glucose concentration variation has the potential to regulate BGLs in real time effectively. In addition, F-insulin also achieved pulsatile insulin release for several cycles by alternating glucose concentrations between 100 and 400 mg/dl (Fig. 3D). Meanwhile, the far-ultraviolet circular dichroism spectra results suggested that the released insulin retained α-helical secondary structure and bioactivity (fig. S3E).

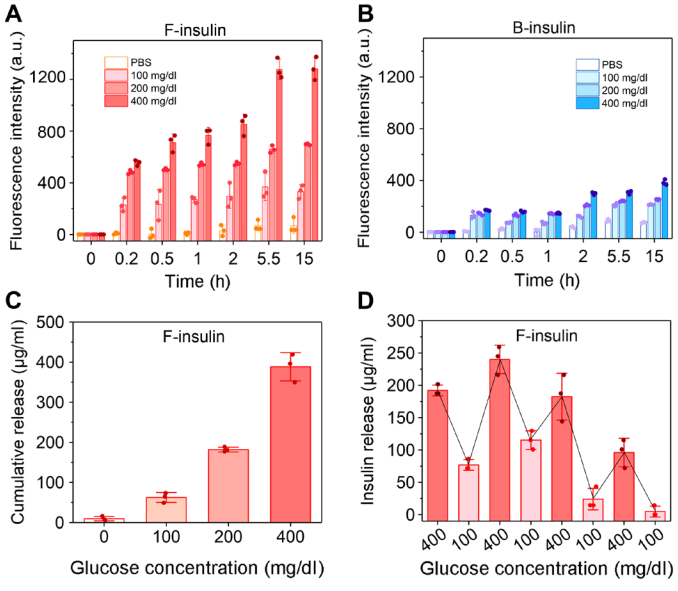

Fig. 3. Glucose- and structure-dependent insulin release. (**A** and **B**) Glucose-dependent insulin release from F-insulin (A) and B-insulin (B) over time. Insulin was labeled with rhodamine B. The glucose concentrations were set to 0, 100, 200, and 400 mg/dl. Data points are means ± SD ($n = 3$). a.u., arbitrary units. (**C**) Cumulative insulin release profile of F-insulin. The complex was incubated in each solution for 10 min. Data points are means ± SD ($n = 3$). (**D**) Pulsatile insulin release from F-insulin by alternating the glucose concentration. The complex was incubated in each solution for 2 min. Data points are means ± SD ($n = 3$).

In vivo evaluation of the complex in diabetic mice

The in vivo therapeutic efficacy of complex was evaluated in type 1 diabetic mouse model induced by streptozotocin (STZ). The diabetic mice were assigned to be treated with either F-insulin, B-insulin, and native insulin at a dose of 80 U/kg or PBS. The BGLs of all treated groups decreased to below 200 mg/dl, indicating the retention of

activity of complexed insulin (Fig. 4A). Moreover, F-insulin was shown to maintain BGLs within the normal range (<200 mg/dl) for more than 8 hours, much longer than native insulin and B-insulin (Fig. 4B). The live imaging results further confirmed the prolonged retention of subcutaneously injected F-insulin as compared with native insulin (Fig. 4C).

Next, the superior release rate of insulin under hyperglycemic conditions from the F-insulin complex was evaluated. A spike of plasma insulin level of approximately 7500 μU/ml was observed at ~30 min after injection of F-insulin (fig. S4A), consistent with the rapid down-regulation of BGLs. The plasma insulin level quickly decreased to approximately 750 μU/ml at 1.5 hours and further

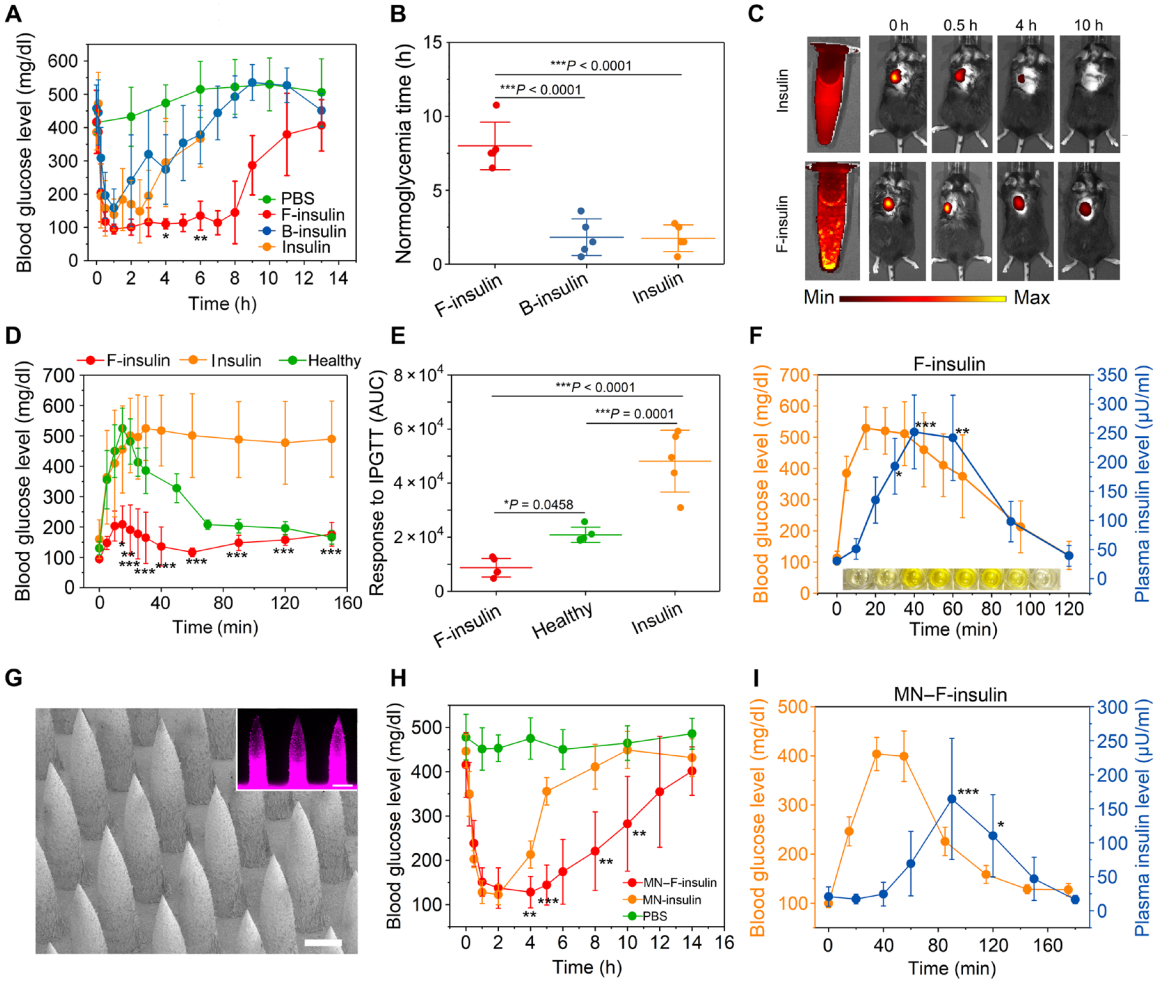

Fig. 4. In vivo evaluation of insulin complex for type 1 diabetic mice treatment. (**A**) BGLs of type 1 diabetic mice treated with subcutaneously injected native insulin, F-insulin, or B-insulin. PBS was used as a control. The insulin-equivalent dose was 80 U/kg. Data points are means ± SD ($n = 5$). Statistical significance between groups treated with F-insulin and native insulin was calculated. (**B**) Normoglycemic time of mice treated with subcutaneously injected F-insulin, B-insulin, and native insulin. Statistical significance was calculated. Data points are means ± SD ($n = 5$). (**C**) Live imaging of subcutaneously injected F-insulin and native insulin labeled with sulfo-Cy5. (**D**) IPGTT in diabetic mice at 3 hours after treatment of F-insulin or native insulin. Glucose dose was set to 1.5 g/kg. Healthy mice were used as control. Data points are means ± SD ($n = 5$). Statistical significance between F-insulin– and native insulin–treated groups was calculated. (**E**) Responsiveness to IPGTT in terms of the area under the curve (AUC) in 150 min, with the baseline set at the 0-min blood glucose reading. Data points are means ± SD ($n = 5$). Statistical significance between groups was calculated. (**F**) In vivo glucose-responsive insulin release triggered by intraperitoneal glucose injection at 4 hours after treatment of F-insulin at a dose of 80 U/kg. Glucose dose was set to 2 g/kg. Data points are means ± SD ($n = 4$ to 5). Statistical significance between the plasma insulin levels at various time points after glucose challenge and that at 0 min was calculated. Inset: Representative image of the resultant light yellow solution associated with enzyme-linked immunosorbent assay (ELISA) measurement. Plasma collected at 0, 10, 20, 30, 40, 60, 90, and 120 min after treatment of F-insulin was added to each well one by one from left to right. 5,5′-Tetramethylbenzidine (TMB) was used as the substrate of horseradish peroxidase, and the addition of sulfuric acid (0.6 N) turned the blue product of TMB to light yellow. (**G**) Representative scanning electron microscopy image of the MN arrays. Inset: Representative fluorescence image of the MNs loaded with F-insulin. Insulin was labeled with rhodamine B. Scale bar, 300 μm. (**H**) BGLs of type 1 diabetic mice treated with MN array patches loaded with insulin (MN-insulin) or F-insulin (MN–F-insulin) (2 mg of insulin per patch). Blank MN loaded with PBS was used as a negative control. One patch was applied to one mouse. Statistical significance between the groups treated with MN-insulin and MN–F-insulin was calculated. Data points are means ± SD ($n = 5$). (**I**) In vivo glucose-responsive insulin release triggered by intraperitoneal glucose injection at 3 hours after treatment of MN array patch load with F-insulin. Each mouse was treated with one patch containing 2 mg of insulin encapsulated in the complex. Glucose was given at 2 g/kg. Data points are means ± SD. ($n = 4$). Statistical significance between the plasma insulin levels at various time points after glucose challenge and that at 0 min was calculated. All the statistical analyses were performed by one-way analysis of variance (ANOVA) with a Tukey post hoc test or Student's *t* test. *$P < 0.05$, **$P < 0.01$, and ***$P < 0.001$.

decreased to 22 μU/ml at 4 hours after treatment, which was essential for maintaining normoglycemia while avoiding hypoglycemia. By comparison, the plasma insulin level of mice treated with B-insulin showed a flat peak of insulin level at 30 min after injection (fig. S4A), which was mainly due to the burst release of loosely adsorbed insulin. However, the fast elimination of insulin from the circulation (*49*) and slow insulin release from B-insulin failed to maintain a therapeutically effective blood insulin level.

Intraperitoneal glucose tolerance tests (IPGTTs) associated with in vivo glucose response were further performed 3 hours after treatment with F-insulin. Blood glucose peaks were observed for all groups after intraperitoneal glucose injection (Fig. 4, D and E), while only the healthy mice and F-insulin–treated diabetic mice reestablished normoglycemia in a brief period. For mice treated with F-insulin, associated with the increase in blood glucose (Fig. 4F), a remarkable spike of plasma insulin (from 30 to 250 μU/ml) (Fig. 4F) was observed, and then it gradually decreased to 39 μU/ml. In contrast, mice treated with insulin glargine, commercialized long-acting insulin, showed no change in plasma insulin level during IPGTT (fig. S4B). This fast in vivo glucose-responsive insulin release kinetics is essential for maintaining normoglycemia when facing glucose challenges. Furthermore, the poly($EDAA_{0.4}$-$FPBA_{0.6}$) used for F-insulin was mainly eliminated from the body through the liver (fig. S4C).

To further demonstrate the potential of glucose-sensitive F-insulin in regulating glycemia over time, insulin complexes were subcutaneously co-injected with in situ–formed absorbable gel [Pluronic F-127 (PF-127)] (*50*). Similar experimental groups were set but with an increased insulin dose (300 U/kg). Compared to other insulin formulations, only F-insulin was found to be able to regulate blood glucose within a normal range for more than 30 hours (fig. S4D). Upon IPGTT, F-insulin loaded in PF-127 could regulate glucose back to normal range rapidly, which was comparable to that of subcutaneously injected F-insulin (fig. S4E). The diabetic mice were further treated continuously for 2 weeks to evaluate the longer-term glucose-regulating efficacy. The diabetic mice receiving F-insulin and insulin glargine were able to maintain their BGLs within the normal range with a longer duration compared to those treated with native insulin (fig. S4F). During the whole treatment, negligible antibodies including immunoglobulin E (IgE), immunoglobulin M (IgM), and immunoglobulin G (IgG) were generated against the subcutaneously injected materials and insulin (fig. S5A). Moreover, negligible changes were observed in blood cell counts, albumin (ALB), aspartate aminotransferase (AST), and blood urea nitrogen (BUN) (fig. S5B). Tissue inflammation and immune response were also studied. Hematoxylin and eosin (H&E) staining results indicated slight neutrophil infiltration on day 3 after administration of F-insulin–loaded PF-127 gel, which was resolved by day 7 (fig. S5C). Masson's trichrome staining results also indicated neutrophil infiltration for PF-127 gel with or without loading F-insulin (fig. S6). However, neutrophil infiltration was limited in F-insulin–treated mice. Furthermore, negligible fibrosis was formed for all treated groups during and after treatment (fig. S6). Consistently, slight macrophage infiltration was observed at the administration site of mice treated with either blank or F-insulin–loaded PF-127 gel on day 3 after treatment (fig. S7).

F-insulin could also be easily loaded into a dissolvable microneedle (MN) array patch made from polyvinylpyrrolidone (PVP) (Fig. 4G). The insulin release from the complex loaded in the MN patch was promoted in the presence of glucose, which is vital for in vivo application of complex-loaded patch (fig. S8A). The glucose levels of type 1 diabetic mice treated with MN–F-insulin slowly decreased to ~100 mg/dl and were maintained below 200 mg/dl for up to 6 hours, much longer than that of mice treated with MN-insulin (Fig. 4H). IPGTT was also carried out at 3 hours after treatment of MN–F-insulin (fig. S8B). Plasma insulin level increased from 20 to 160 μU/ml, associated with a spike in BGLs (Fig. 4I), and then gradually decreased to 16 μU/ml.

In vivo evaluation of the complex in diabetic pigs

The diabetes treatment efficacy of F-insulin was further evaluated in a STZ-induced diabetic Göttingen minipig model using a continuous glucose monitoring system (CGMS). Similar to the results obtained in diabetic mice, F-insulin showed significantly prolonged BGL-regulating effect in pigs as compared with native insulin (Fig. 5A). The BGLs of each pig treated with F-insulin displayed a relatively "flat" stage around 100 mg/dl during the treatment, likely due to the enhanced insulin release from F-insulin when the BGLs gradually increased from 40 mg/ml to 100 mg/dl. As shown, the BGLs may fall below 40 mg/dl that could not be read in detail by CGMS due to its detection limit. In normal pigs, glucose levels below 40 mg/dl are common and well described using CGMS (*51*). Furthermore, pigs were carefully watched during the treatment, with sampled blood monitored with a blood glucose meter (table S1). No symptoms of hypoglycemia were identified. In addition, oral glucose tolerance tests were carried out at an insulin dose of 0.5 U/kg. The subsequent glucose challenge led to an immediate increase of BGLs to the upper detection limit of CGMS if the pigs were treated with insulin (Fig. 5B). In contrast, the insulin complex treatment obviously inhibited the increase of BGLs. Furthermore, intravenously infused dextrose solution led to a sharp increase of BGLs, which effectively induced spikes of accompanying serum insulin for F-insulin–treated diabetic pigs (Fig. 5C), while no C-peptide (pig) spikes were observed (fig. S9A). In contrast, only a steady decrease of insulin level was observed due to clearance when the diabetic minipigs were treated with native insulin (fig. S9, B to D), substantiating that the serum insulin spikes of complex-treated minipigs were achieved because of the glucose-triggered insulin release.

DISCUSSION

To achieve glucose-responsive insulin release in vivo in a fast manner, we conceived the concept of engineering a positively charged polymer integrated with a glucose-sensing moiety, which could switch the positive charge of polymer to negative in response to increased glucose concentration. At neutral physiological pH, the prepared positively charged polymer can form a micro-sized stable water-insoluble complex with insulin that could be injected subcutaneously. After adjusting the polymer structure and the ratio between polymer and insulin, an optimized complex (F-insulin) was obtained, showing robust glucose-dependent insulin release profile. In a type 1 diabetic mouse model, the complex showed prolonged blood glucose–regulating ability as compared to native insulin, while negligible hypoglycemia was observed at the dose studied. In addition, no obvious IgE, IgM, and IgG in response to F-insulin were generated during the whole treatment. Further long-term toxicity evaluation should be performed for potential translation.

This glucose-responsive formulation could be useful for controlling postprandial glucose levels, as it could increase the time window to start and complete a meal after administration. An acute glucose injection triggered a quick elevation of plasma insulin level associated with the blood glucose spike. The insulin level also decreased back to

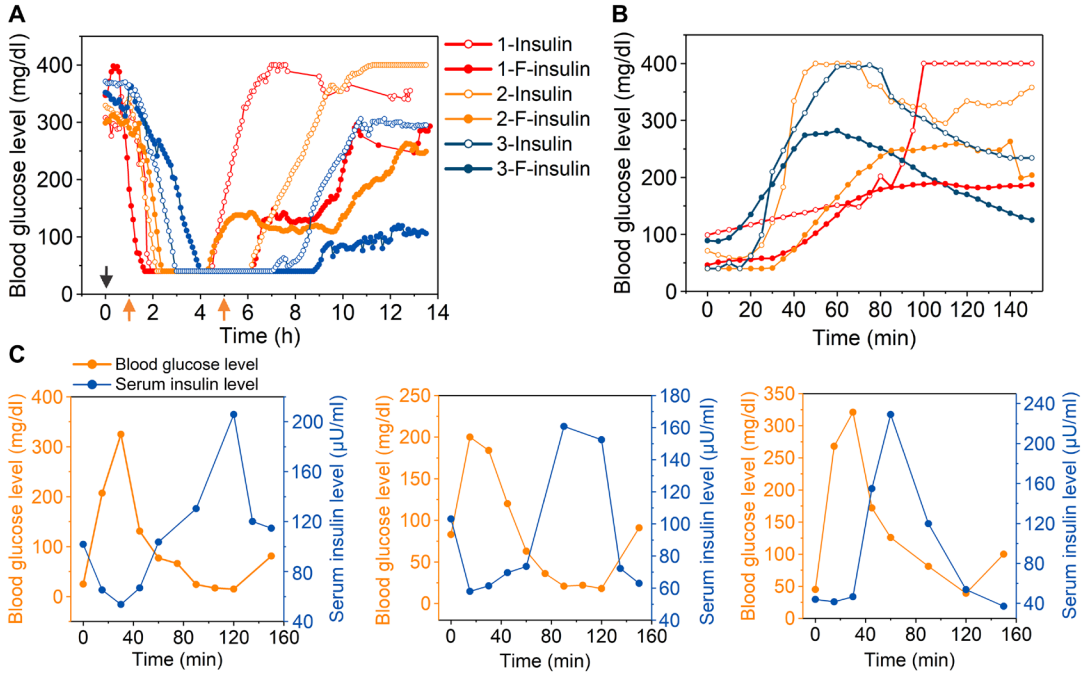

Fig. 5. In vivo evaluation of F-insulin for treatment of type 1 diabetic minipig. (**A**) BGLs of type 1 diabetic minipigs treated with native insulin or F-insulin. The insulin dose was set to 1 U/kg. The BGLs were measured continuously by CGMS. Each curve represents the BGL change obtained from a single minipig. The same color indicated the data from the same pig. Three pigs (designated as 1, 2, or 3) were used in this study. The black arrow indicated the injection of insulin or F-insulin. The orange arrows indicated the two meals for pigs. (**B**) Oral glucose tolerance test toward diabetic minipigs at 4 hours after treatment of F-insulin (0.5 U/kg). Glucose was given at 0.5 g/kg. (**C**) Intravenous glucose tolerance test in diabetic minipigs at 4 hours after treatment of F-insulin at a dose of 1 U/kg. Dextrose solution (5%) was intravenously infused at a dose of 0.75 g/kg. The rate of infusion was set to 1 liter/hour. Figures from left to right indicated pigs 1, 2, and 3, respectively.

basal levels after the BGL normalized, which could minimize the potential for hypoglycemia. While the results in diabetic mice were encouraging, prolonged glucose regulation was also demonstrated in the diabetic minipigs, verifying the sustained release of insulin from the complex. Intravenously infused dextrose raised the BGLs of F-insulin–treated diabetic minipigs, triggering insulin release. For future translation, as demonstrated, this complex formulation can be integrated with an injectable gel matrix for sustained long-term insulin release or a transdermal MN array patch for painless and disposable administration.

MATERIALS AND METHODS

Materials

Ethylenediamine, di-tert-butyl decarbonate (Boc_2O), acryloyl chloride, 2,2′-azobis(2-methylpropionitrile) (AIBN), tetrahydrofuran (THF), trifluoroacetic acid (TFA), dichloromethane (CH_2Cl_2), NHS, and *N*-(3-dimethylaminopropyl)-*N*′-ethylcarbodiimide hydrochloride (EDC•HCl) were purchased from Sigma-Aldrich. 4-Carboxy-3-florobenzeneboronic acid and 4-carboxybenzeneboronic acid were obtained from Fisher Scientific. Insulin used in this study was recombinant human insulin purchased from Thermo Fisher Scientific (catalog no. A11382IJ). Both weight unit "mg" and international unit "U" were used for insulin. Unless mentioned otherwise, all the reactions were carried out with the protection of N_2 atmosphere.

Methods

Synthesis of Boc-EDA

Ethylenediamine (14 ml) was dissolved in $CHCl_3$ (200 ml) and cooled in an ice bath. Boc_2O (4.1 g) dissolved in $CHCl_3$ (50 ml) was added dropwise for 3 hours, and the reaction was stirred overnight at room temperature. After filtration, the solution was washed with saturated NaCl aqueous solution (3 × 50 ml), dried over anhydrous $MgSO_4$, filtrated, and evaporated to obtain a colorless oil. This liquid was used without further purification.

Synthesis of Boc-EDAA

Boc-EDA (1.6 g, 10 mmol) was dissolved in H_2O (50 ml) and filtrated to obtain a clear solution, to which acryloyl chloride (1.5 g, 16 mmol) in THF (20 ml) was added. $NaHCO_3$ (1.5 g) was then added slowly to the solution, and the reaction was stopped after an additional 30 min. The mixture was extracted using CH_2Cl_2 (3 × 50 ml), dried over anhydrous $MgSO_4$, and filtrated. After evaporation of the solvent, white Boc-EDAA (1.6 g, yield 70%) was obtained. ^{1}H NMR (400 MHz, in $CDCl_3$, δ): 6.54 (s, 1H), 6.22 (d, 1H), 6.1 (q, 1H), 5.6 (d, 1H), 5.02 (s, 1H), 3.4 (q, 2H), 3.3 (s, 2H), and 1.42 (s, 9H).

Synthesis of poly(Boc-EDAA)

Boc-EDAA (0.5 g) and AIBN (12 mg) were mixed and dissolved in THF (2 ml), which was purged with N_2 for 10 min. After incubation at 60°C overnight, the reaction mixture was diluted with THF (10 ml), added to water, and dialyzed against water (3 × 4 L). Last, the water was lyophilized, and a white solid was obtained (0.45 g, yield 90%).

Synthesis of poly(EDAA)

Poly(Boc-EDAA) (0.3 g) was added to CH_2Cl_2 (10 ml) containing TFA (3 ml) and stirred for 2 hours. After removing the solvent, the residual was dialyzed against water (3 × 4 liters) and lyophilized to obtain poly(EDAA) (0.2 g, yield 90%) as a slightly yellow solid.

Synthesis of PBA-NHS

4-Carboxyphenylboronic acid (2 g, 12 mmol) and NHS (2 g, 17 mmol) were mixed in dimethylformamide (DMF) (100 ml) and cooled in an

ice bath while stirring. EDC•HCl (3 g, 18 mmol) was added, and the reaction was stirred overnight at room temperature. The mixture was poured into CH_2Cl_2 (200 ml), washed with HCl (0.1 N, 3 × 50 ml) and $NaHCO_3$ (0.1 N, 3 × 50 ml) successively, and dried over anhydrous $MgSO_4$. The solvent was evaporated under reduced pressure, and a pure white PBA-NHS was obtained (3 g, yield 90%). ^{1}H NMR [400 MHz, in dimethyl sulfoxide (DMSO)–d_6, δ]: 8.43 (s, 2H), 8.02 (t, 4H), and 2.88 (s, 4H).

Synthesis of FPBA-NHS

FPBA (2 g, 12 mmol) and NHS (2 g, 17 mmol) were mixed in DMF (100 ml) and cooled in an ice bath while stirring. EDC•HCl (3 g, 18 mmol) was added, and the reaction was stirred overnight at room temperature. The mixture was poured into CH_2Cl_2 (200 ml), washed with HCl (0.1 N, 3 × 50 ml) and $NaHCO_3$ (0.1 N, 3 × 50 ml) successively, and dried over anhydrous $MgSO_4$. The solvent was evaporated under reduced pressure, and a pure white FPBA-NHS was obtained (2.7 g, yield 80%). ^{1}H NMR (400 MHz, in DMSO-d_6, δ): 8.59 (s, 2H), 8.0 (t, 1H), 7.79 (q, 2H), and 2.9 (s, 4H).

Synthesis of FPBA-modified poly(EDAA), with poly($EDAA_{0.4}$-$FPBA_{0.6}$) as an example

Poly(EDAA) (0.15 g) was dissolved in deionized water (10 ml). FPBA-NHS (220 mg) dissolved in DMSO (2 ml) was added to give a clear solution. Then, solid $NaHCO_3$ was added slowly to maintain the pH around 7.2, and the reaction was stirred for 30 min. Last, the mixture was dialyzed against deionized water (3 × 4 liters) and subsequently lyophilized to give a white solid (0.3 g, yield 80%).

Synthesis of RhB-insulin

Rhodamine B isothiocyanate (1 mg) dissolved in DMSO (1 ml) was added to the aqueous solution of insulin (100 mg). Solid $NaHCO_3$ was added carefully to adjust the solution to pH 8, and the reaction was further stirred overnight. Then, the mixture was dialyzed against deionized H_2O (3 × 4 liters) and lyophilized to obtain RhB-insulin.

Preparation of polymer nanoparticles

Poly($EDAA_{0.4}$-$FPBA_{0.6}$) (1 mg) was dissolved in acidified deionized H_2O (50 μl). Upon rapid addition of PBS (10 mM, pH 7.4, 1 ml) to this solution, the polymer precipitated and formed stable nanoparticles. Nanoparticle solution from poly($EDAA_{0.4}$-$PBA_{0.6}$) was prepared by the same method.

Preparation of insulin complex

We described the preparation of poly($EDAA_{0.4}$-$FPBA_{0.6}$)–insulin complex as an example. Both insulin (1 mg, 28.8 U) and poly($EDAA_{0.4}$-$FPBA_{0.6}$) (1 mg) were dissolved in acidified H_2O (50 μl) and mixed. NaOH aqueous solution (0.1 N) was added carefully, and the pH was finely tuned to 7.4 until a white precipitate formed. To this suspension, PBS (10 mM, pH 7.4, 1 ml) was added, and the mixture was centrifuged. The precipitate was further washed for several times with PBS. Last, the suspension was kept in PBS 7.4 and used directly for further experiment. The insulin loading capacity (LC) is defined as LC = A/B, and the loading efficiency (LE) is defined as LE = A/C, where A is the amount of insulin loaded in complex, B is the total weight of complex, and C is the insulin amount used.

Size and ζ potential of nanoparticles

The size and ζ potential of nanoparticles were measured on a Zetasizer instrument (Malvern). The impact of glucose concentration on the ζ potential of nanoparticles was determined by adding various amounts of glucose (0.3 g/ml) to the solution of nanoparticles, which stood for 2 min before taking the measurement. Nanoparticles of poly($EDAA_{0.4}$-$FPBA_{0.6}$) would precipitate when glucose was added to 400 mg/dl, and rapid ascertainment of this measurement was critical.

Observation of polymer nanoparticles by TEM

Nanoparticle aqueous solution (0.5 mg/ml, 10 μl) was dropped onto a copper grip and stayed for 30 min before a filtrate paper was used to remove the residual solution. Then, uranyl acetate solution (5%, 10 μl) was added onto the copper grip and stayed for 10 min, and a filtrate paper was also used to remove the solution. After further drying for 1 hour, the sample was observed on a JEOL 2000FX TEM.

The glucose adsorption study

Insulin complexes, composed of insulin (1 mg, 28.8 U) and polymer (1 mg), were suspended in PBS 7.4 (1 ml), to which glucose (0.3 g/ml) was added to acquire various glucose concentrations (100, 200, or 400 mg/dl). This mixture was incubated at 37°C, and the glucose concentration in the supernatant was monitored with a Clarity GL2Plus glucose meter. The concentration was calculated according to a standard curve.

In vitro insulin release study

Briefly, insulin (1 mg, 28.8 U) loaded in complexes of different polymers was allocated to centrifuge tubes containing PBS (pH 7.4, 1 ml), and various amounts of glucose (0.3 g/ml) were added to prepare different concentrations (0, 100, 200, and 400 mg/dl). Then, the centrifuge tubes were incubated at 37°C and vibrated. At timed intervals, a clear supernatant solution (10 μl) collected through centrifuge was further added to Coomassie blue (200 μl). The absorbance of the solution was measured at 595 nm, and the concentration was calibrated using an established standard curve. In other cases, RhB-insulin was used, and the fluorescence intensity was recorded at 580 nm (excited at 540 nm).

Animal study

The animal (both mice and minipig) study was approved by the Institutional Animal Care and Use Committee at North Carolina State University and the University of North Carolina at Chapel Hill. The C57BL/6J mice were maintained in a specific pathogen–free room with a 12:12 light-dark cycle. The diabetic mouse model was induced using STZ. Typically, after overnight fasting, male C57BL/6J mice (6 to 8 weeks old) were intraperitoneally injected with STZ (150 mg/kg). After 1 week, the mice with fasting blood glucose higher than 300 mg/dl were confirmed as type 1 diabetic mice, which were used for further experiment. During the treatment experiment, the diabetic mice were normally fed with food, and the experiments were started in the morning.

Blood glucose control study in type 1 diabetic mice

Diabetic mice were allocated to different groups and treated with subcutaneously injected native insulin or complexes at an insulin-equivalent dose of 80 U/kg or complex-loaded in PF-127 gel at an insulin-equivalent dose of 300 U/kg. The BGLs were monitored with a Clarity GL2Plus glucose meter. PF-127 was prepared as 50% in aqueous solution, and the complex was suspended in the gel. Before injection, the gel was kept at 4°C for improving fluidity to facilitate subcutaneous injection. For the 2-week-long treatment, the diabetic mice were treated at a dose of 80 U/kg, with two injections (9 a.m. and 6 p.m.) each day.

Plasma insulin level measurement

The plasma insulin level was measured by collecting 20 μl of plasma, which was stored at −20°C until measurement using a human insulin enzyme-linked immunosorbent assay (ELISA) kit (Invitrogen, USA).

Biodistribution study

Fluorescence imaging of the diabetic mice treated with either subcutaneously injected native insulin labeled with sulfo-Cy5 or F-insulin composed of sulfo-Cy5–labeled insulin was measured with the IVIS Spectrum Imaging System (PerkinElmer). The mice were

anesthetized using isoflurane. Poly($EDAA_{0.4}$-$FPBA_{0.6}$) was also labeled with Cy5 and mixed with unlabeled insulin for subcutaneous injection (80 U/kg). At the predetermined time points (1, 3, 8, 24, 48, and 96 hours) after treatment, the mice were euthanized, and the primary organs were collected for imaging with the IVIS Spectrum Imaging System.

Intraperitoneal glucose tolerance test

Diabetic mice were allocated to different groups and treated with subcutaneously injected native insulin or complexes at a dose of 80 U/kg. Then, glucose (0.4 g/ml) was given at 3 hours after treatment at a dose of 1.5 g/kg, and BGLs were monitored with a Clarity GL2Plus glucose meter. For IPGTT-triggered insulin release from subcutaneous insulin depot, glucose (2 g/kg) was given at 4 hours after treatment of subcutaneously injected insulin glargine (80 U/kg) or F-insulin (80 U/kg) to achieve a clear spike of blood glucose. Blood (50 μl) was collected at predetermined intervals, centrifuged to isolate plasma, and stored at −20°C until measurement.

Preparation of complex-loaded MN patch

Poly($EDAA_{0.4}$-$FPBA_{0.6}$) (10 mg) and insulin (10 mg) were mixed to prepare F-insulin suspension, which was further allocated to five MN patch molds (20 × 20; base: 300 μm, circle; body: 900 μm, with 600-μm cylindrical body and 300-μm conical tip), and dried under vacuum. Then, PVP [10 weight % (wt %), 100 μl] was placed on the MN molds and incubated under vacuum again to let the solution get into the MN holes, followed by the addition of another 500 μl of PVP (10 wt %) solution. Then, the MN patch molds were placed under vacuum until dry. The MN array patch was observed on a scanning electron microscope (FEI Verios 460L).

In vivo study using MN array patch

Diabetic mice were allocated to different groups and treated with MN array patch loaded with complex or native insulin at an insulin-equivalent dose of 2 mg per mouse. The BGLs were monitored with a Clarity GL2Plus glucose meter. The plasma insulin levels were measured by collecting 50 μl of blood, and the plasma was isolated and stored at −20°C until measurement. For IPGTT-triggered insulin release, glucose (0.4 g/ml, 2 g/kg) was given at 3 hours after treatment of F-insulin loaded in MN array patch.

Glucose control studies of complexes using STZ-induced diabetic minipigs

All pig studies were carefully monitored by veterinarians to deal with potential hypoglycemia. Göttingen minipigs (6 months old) were injected with STZ (150 mg/kg) to establish the diabetic minipig model. Three diabetic pigs (35, 32, and 28 kg for pigs 1, 2, and 3, respectively) were treated with subcutaneously injected native insulin or complex at a dose of 1 U/kg after overnight fasting, and then two meals are provided normally during the treatment. The BGLs were continuously monitored using a CGMS (Dexcom G4).

Oral glucose tolerance tests in diabetic pigs

Three diabetic pigs were treated with subcutaneously injected native insulin or complex at a dose of 0.5 U/kg after overnight fasting, and then glucose (0.5 g/kg) was given at 4 hours after treatment. The BGLs were continuously monitored using a CGMS.

Intravenous glucose administration triggered insulin release

Three diabetic pigs were treated with subcutaneously injected native insulin or complex at a dose of 1 U/kg after overnight fasting. Four hours later, dextrose (5 wt %) solution was infused at a dose of 0.75 g/kg at a rate of 1 liter/hour, while the pigs were kept anesthetized using isoflurane. Blood was collected from external jugular vein before and during the experiment at predetermined intervals to measure BGLs. In addition, serum was also collected from the blood samples using a serum separator tube (BD) for subsequent insulin level measurement using Iso-Insulin ELISA (Mercodia).

H&E staining experiment

The inflammation caused by subcutaneous injection of the complex-loaded PF-127 gel was evaluated. After the removal of the back hair, diabetic mice were subcutaneously injected with PF-127 (100 μl) loaded with insulin complex (300 U/kg). On day 3 or 7 after injection, mice were euthanized, and pieces of skin from the treated or untreated sites were collected and fixed in 4% formaldehyde and proceeded for H&E staining. The images were taken using a microscope (Olympus).

Masson's trichrome staining and macrophage staining

Diabetic mice were subcutaneously injected with F-insulin (80 U/kg), PF-127 (blank), or PF-127 gel loaded with F-insulin (300 U/kg). At the predetermined time point, the diabetic mice were euthanized, and the skin from the treated sites was collected. Part of each piece of the skin was fixed in 4% formaldehyde and proceeded for Masson's trichrome staining. The images were taken using a microscope (LAXCO, LMI6-PH2). The skin left was subject to cryosection (10 μm) and proceeded for macrophage staining. The macrophage was stained with rat monoclonal antibody to F4/80 purchased from Abcam (lot no. GR3250648-1) and Alexa Fluor 488–labeled goat polyclonal antibody to rat IgG purchased from Abcam (lot no. GR3234544-1). The macrophage was shown in green. The nuclei were stained with 4′,6-diamidino-2-phenylindole (DAPI) and shown in blue. The fluorescence image was observed on a confocal microscope (Zeiss LSM710).

Host response and toxicity evaluation

Diabetic mice were continuously treated with F-insulin (80 U/kg), native insulin (80 U/kg), insulin glargine (80 U/kg), or PBS for 2 weeks. Each mouse received two injections per day (9 a.m. and 6 p.m.). The serum was collected for evaluating the immunoglobin levels using ELISA purchased from Abcam (catalog nos. ab157719, ab215085, and ab157718). Whole blood was also obtained for complete blood count, while AST, ALB, and BUN in serum were detected for evaluating toxicity toward the liver and kidney.

Statistical analysis

All data were shown as the means ± SD. One-way analysis of variance (ANOVA) with Tukey post hoc tests was used to carry out multiple comparisons, while Student's *t* test was used to analyze the difference between two groups.

SUPPLEMENTARY MATERIALS

Supplementary material for this article is available at http://advances.sciencemag.org/cgi/content/full/5/7/eaaw4357/DC1

Scheme S1. Synthesis route of polymers.
Fig. S1. Characterization of the complex.
Fig. S2. ^{1}H NMR spectra of various compounds synthesized.
Fig. S3. In vitro insulin release studies.
Fig. S4. Evaluation of insulin complexes in type 1 diabetic mice.
Fig. S5. Host response and toxicity evaluation in diabetic mice.
Fig. S6. The Masson's trichrome staining sections of the skin with or without treatment.
Fig. S7. The immunofluorescence staining sections of the skin with or without treatment.
Fig. S8 Characterization of MN array patch.
Fig. S9. Glucose challenge study in diabetic minipigs.
Table S1. The BGLs of diabetic pigs.

REFERENCES AND NOTES

1. Y. Ohkubo, H. Kishikawa, E. Araki, T. Miyata, S. Isami, S. Motoyoshi, Y. Kojima, N. Furuyoshi, M. Shichiri, Intensive insulin therapy prevents the progression of diabetic microvascular

complications in Japanese patients with non-insulin-dependent diabetes-mellitus: A randomized prospective 6-year study. *Diabetes Res. Clin. Pract.* **28**, 103–117 (1995).
2. R. Mo, T. Jiang, J. Di, W. Tai, Z. Gu, Emerging micro- and nanotechnology based synthetic approaches for insulin delivery. *Chem. Soc. Rev.* **43**, 3595–3629 (2014).
3. O. Veiseh, B. C. Tang, K. A. Whitehead, D. G. Anderson, R. Langer, Managing diabetes with nanomedicine: Challenges and opportunities. *Nat. Rev. Drug Discov.* **14**, 45–57 (2015).
4. J. Yu, Y. Zhang, H. Bomba, Z. Gu, Stimuli-responsive delivery of therapeutics for diabetes treatment. *Bioeng. Transl. Med.* **1**, 323–337 (2016).
5. Y. Zhao, B. G. Trewyn, I. I. Slowing, V. S.-Y. Lin, Mesoporous silica nanoparticle-based double drug delivery system for glucose-responsive controlled release of insulin and cyclic AMP. *J. Am. Chem. Soc.* **131**, 8398–8400 (2009).
6. H.-W. Sung, K. Sonaje, Z.-X. Liao, L.-W. Hsu, E.-Y. Chuang, pH-responsive nanoparticles shelled with Chitosan for oral delivery of insulin: From mechanism to therapeutic applications. *Acc. Chem. Res.* **45**, 619–629 (2012).
7. S. Payyappilly, S. Dhara, S. Chattopadhyay, Thermoresponsive biodegradable PEG-PCL-PEG based injectable hydrogel for pulsatile insulin delivery. *J. Biomed. Mater. Res. A* **102**, 1500–1509 (2014).
8. J. Di, J. Yu, Q. Wang, S. Yao, D. Suo, Y. Ye, M. Pless, Y. Zhu, Y. Jing, Z. Gu, Ultrasound-triggered noninvasive regulation of blood glucose levels using microgels integrated with insulin nanocapsules. *Nano Res.* **10**, 1393–1402 (2017).
9. J. Kost, K. Leong, R. Langer, Ultrasound-enhanced polymer degradation and release of incorporated substances. *Proc. Natl. Acad. Sci. U.S.A.* **86**, 7663–7666 (1989).
10. S. Mitragotri, D. Blankschtein, R. Langer, Ultrasound-mediated transdermal protein delivery. *Science* **269**, 850–853 (1995).
11. J. Di, S. Yao, Y. Ye, Z. Cui, J. Yu, T. K. Ghosh, Y. Zhu, Z. Gu, Stretch-triggered drug delivery from wearable elastomer films containing therapeutic depots. *ACS Nano* **9**, 9407–9415 (2015).
12. N. Rasool, T. Yasin, J. Y. Y. Heng, Z. Akhter, Synthesis and characterization of novel pH-, ionic strength and temperature-sensitive hydrogel for insulin delivery. *Polymer* **51**, 1687–1693 (2010).
13. O. Saslawski, C. Weingarten, J. P. Benoit, P. Couvreur, Magnetically responsive microspheres for the pulsed delivery of insulin. *Life Sci.* **42**, 1521–1528 (1988).
14. B. P. Timko, M. Arruebo, S. A. Shankarappa, J. B. McAlvin, O. S. Okonkwo, B. Mizrahi, C. F. Stefanescu, L. Gomez, J. Zhu, A. Zhu, J. Santamaria, R. Langer, D. S. Kohane, Near-infrared–actuated devices for remotely controlled drug delivery. *Proc. Natl. Acad. Sci. U.S.A.* **111**, 1349–1354 (2014).
15. N. A. Bakh, A. B. Cortinas, M. A. Weiss, R. S. Langer, D. G. Anderson, Z. Gu, S. Dutta, M. S. Strano, Glucose-responsive insulin by molecular and physical design. *Nat. Chem.* **9**, 937–943 (2017).
16. Y. Lu, A. A. Aimetti, R. Langer, Z. Gu, Bioresponsive materials. *Nat. Rev. Mater.* **2**, 16075 (2016).
17. Y. Ito, M. Casolaro, K. Kono, Y. Imanishi, An insulin-releasing system that is responsive to glucose. *J. Control. Release* **10**, 195–203 (1989).
18. C. R. Gordijo, K. Koulajian, A. J. Shuhendler, L. D. Bonifacio, H. Y. Huang, S. Chiang, G. A. Ozin, A. Giacca, X. Y. Wu, Nanotechnology-enabled closed loop insulin delivery device: In vitro and in vivo evaluation of glucose-regulated insulin release for diabetes control. *Adv. Funct. Mater.* **21**, 73–82 (2011).
19. K. Podual, F. J. Doyle III, N. A. Peppas, Glucose-sensitivity of glucose oxidase-containing cationic copolymer hydrogels having poly(ethylene glycol) grafts. *J. Control. Release* **67**, 9–17 (2000).
20. K. Podual, F. J. Doyle III, N. A. Peppas, Preparation and dynamic response of cationic copolymer hydrogels containing glucose oxidase. *Polymer* **41**, 3975–3983 (2000).
21. N. A. Peppas, Y. Huang, M. Torres-Lugo, J. H. Ward, J. Zhang, Physicochemical, foundations and structural design of hydrogels in medicine and biology. *Annu. Rev. Biomed. Eng.* **2**, 9–29 (2000).
22. M. Brownlee, A. Cerami, A glucose-controlled insulin-delivery system: Semisynthetic insulin bound to lectin. *Science* **206**, 1190–1191 (1979).
23. M. Brownlee, A. Cerami, Glycosylated insulin complexed to Concanavalin A. Biochemical basis for a closed-loop insulin delivery system. *Diabetes* **32**, 499–504 (1983).
24. A. A. Obaidat, K. Park, Characterization of glucose dependent gel-sol phase transition of the polymeric glucose-Concanavalin A hydrogel system. *Pharm. Res.* **13**, 989–995 (1996).
25. C. Wang, Y. Q. Ye, W. J. Sun, J. C. Yu, J. Q. Wang, D. S. Lawrence, J. B. Buse, Z. Gu, Red blood cells for glucose-responsive insulin delivery. *Adv. Mater.* **29**, 1606617 (2017).
26. Y. Dong, W. Wang, O. Veiseh, E. A. Appel, K. Xue, M. J. Webber, B. C. Tang, X.-W. Yang, G. C. Weir, R. Langer, D. G. Anderson, Injectable and glucose-responsive hydrogels based on boronic acid–glucose complexation. *Langmuir* **32**, 8743–8747 (2016).
27. D. H.-C. Chou, M. J. Webber, B. C. Tang, A. B. Lin, L. S. Thapa, D. Deng, J. V. Truong, A. B. Cortinas, R. Langer, D. G. Anderson, Glucose-responsive insulin activity by covalent modification with aliphatic phenylboronic acid conjugates. *Proc. Natl. Acad. Sci. U.S.A.* **112**, 2401–2406 (2015).
28. A. Matsumoto, T. Kurata, D. Shiino, K. Kataoka, Swelling and shrinking kinetics of totally synthetic, glucose-responsive polymer gel bearing phenylborate derivative as a glucose-sensing moiety. *Macromolecules* **37**, 1502–1510 (2004).
29. D. Shiino, Y. Murata, A. Kubo, Y. J. Kim, K. Kataoka, Y. Koyama, A. Kikuchi, M. Yokoyama, Y. Sakurai, T. Okano, Amine containing phenylboronic acid gel for glucose-responsive insulin release under physiological pH. *J. Control. Release* **37**, 269–276 (1995).
30. A. Matsumoto, R. Yoshida, K. Kataoka, Glucose-responsive polymer gel bearing phenylborate derivative as a glucose-sensing moiety operating at the physiological pH. *Biomacromolecules* **5**, 1038–1045 (2004).
31. K. Kataoka, H. Miyazaki, M. Bunya, T. Okano, Y. Sakurai, Totally synthetic polymer gels responding to external glucose concentration: Their preparation and application to on-off regulation of insulin release. *J. Am. Chem. Soc.* **120**, 12694–12695 (1998).
32. W. L. A. Brooks, B. S. Sumerlin, Synthesis and applications of boronic acid-containing polymers: From materials to medicine. *Chem. Rev.* **116**, 1375–1397 (2016).
33. A. Matsumoto, M. Tanaka, H. Matsumoto, K. Ochi, Y. Moro-oka, H. Kuwata, H. Yamada, I. Shirakawa, T. Miyazawa, H. Ishii, K. Kataoka, Y. Ogawa, Y. Miyahara, T. Suganami, Synthetic "smart gel" provides glucose-responsive insulin delivery in diabetic mice. *Sci. Adv.* **3**, eaaq0723 (2017).
34. A. Matsumoto, T. Ishii, J. Nishida, H. Matsumoto, K. Kataoka, Y. Miyahara, A Synthetic approach toward a self-regulated insulin delivery system. *Angew. Chem. Int. Ed. Engl.* **51**, 2124–2128 (2012).
35. Z. Gu, T. T. Dang, M. Ma, B. C. Tang, H. Cheng, S. Jiang, Y. Dong, Y. Zhang, D. G. Anderson, Glucose-responsive microgels integrated with enzyme nanocapsules for closed-loop insulin delivery. *ACS Nano* **7**, 6758–6766 (2013).
36. Z. Gu, A. A. Aimetti, Q. Wang, T. T. Dang, Y. Zhang, O. Veiseh, H. Cheng, R. S. Langer, D. G. Anderson, Injectable nano-network for glucose-mediated insulin delivery. *ACS Nano* **7**, 4194–4201 (2013).
37. K. Podual, F. J. Doyle III, N. A. Peppas, Dynamic behavior of glucose oxidase-containing microparticles of poly(ethylene glycol)-grafted cationic hydrogels in an environment of changing pH. *Biomaterials* **21**, 1439–1450 (2000).
38. K. Ishihara, M. Kobayashi, N. Ishimaru, I. Shinohara, Glucose-induced permeation control of insulin through a complex membrane consisting of immobilized glucose-oxidase and a poly(amine). *Polym. J.* **16**, 625–631 (1984).
39. J. Yu, Y. Zhang, Y. Ye, R. DiSanto, W. Sun, D. Ranson, F. S. Ligler, J. B. Buse, Z. Gu, Microneedle-array patches loaded with hypoxia-sensitive vesicles provide fast glucose-responsive insulin delivery. *Proc. Natl. Acad. Sci. U.S.A.* **112**, 8260–8265 (2015).
40. J. Yu, C. Qian, Y. Zhang, Z. Cui, Y. Zhu, Q. Shen, F. S. Ligler, J. B. Buse, Z. Gu, Hypoxia and H_2O_2 dual-sensitive vesicles for enhanced glucose-responsive insulin delivery. *Nano Lett.* **17**, 733–739 (2017).
41. X. L. Hu, J. C. Yu, C. G. Qian, Y. Lu, A. R. Kahkoska, Z. G. Xie, X. B. Jing, J. B. Buse, Z. Gu, H_2O_2-responsive vesicles integrated with transcutaneous patches for glucose-mediated insulin delivery. *ACS Nano* **11**, 613–620 (2017).
42. J. Wang, Y. Ye, J. Yu, A. R. Kahkoska, X. Zhang, C. Wang, W. Sun, R. D. Corder, Z. Chen, S. A. Khan, J. B. Buse, Z. Gu, Core-shell microneedle gel for self-regulated insulin delivery. *ACS Nano* **12**, 2466–2473 (2018).
43. R. P. N. Veregin, M. K. Georges, P. M. Kazmaier, G. K. Hamer, Free radical polymerizations for narrow polydispersity resins: Electron spin resonance studies of the kinetics and mechanism. *Macromolecules* **26**, 5316–5320 (1993).
44. T. Reschel, C. Konak, D. Oupicky, L. W. Seymour, K. Ulbrich, Physical properties and in vitro transfection efficiency of gene delivery vectors based on complexes of DNA with synthetic polycations. *J. Control. Release* **81**, 201–217 (2002).
45. W. Park, D. Kim, H. C. Kang, Y. H. Bae, K. Na, Multi-arm histidine copolymer for controlled release of insulin from poly(lactide-co-glycolide) microsphere. *Biomaterials* **33**, 8848–8857 (2012).
46. L. B. Ren, Z. Liu, Y. C. Liu, P. Dou, H.-Y. Chen, Ring-opening polymerization with synergistic co-monomers: Access to a boronate-functionalized polymeric monolith for the specific capture of *cis*-diol-containing biomolecules under neutral conditions. *Angew. Chem. Int. Ed. Engl.* **48**, 6704–6707 (2009).
47. L. Liang, Z. Liu, A self-assembled molecular team of boronic acids at the gold surface for specific capture of cis-diol biomolecules at neutral pH. *Chem. Commun.* **47**, 2255–2257 (2011).
48. G. Springsteen, B. H. Wang, A detailed examination of boronic acid-diol complexation. *Tetrahedron* **58**, 5291–5300 (2002).
49. J. C. Cresto, R. L. Lavine, M. L. Buchly, J. C. Penhos, S. J. Bhathena, L. Recant, Half life of injected ^{125}I-insulin in control and ob/ob mice. *Acta Physiol. Lat. Am.* **27**, 7–15 (1977).
50. Z. Chen, J. Wang, W. Sun, E. Archibong, A. R. Kahkoska, X. Zhang, Y. Lu, F. S. Ligler, J. B. Buse, Z. Gu, Synthetic beta cells for fusion-mediated dynamic insulin secretion. *Nat. Chem. Biol.* **14**, 86–93 (2018).
51. A. Strauss, V. Moskalenko, C. Tiurbe, I. Chodnevskaja, S. Timm, V. A. Wiegering, C.-T. Germer, K. Ulrichs, Goettingen minipigs (GMP): Comparison of two different models for inducing diabetes. *Diabetol. Metab. Syndr.* **4**, 7 (2012).

Acknowledgments
Funding: This work was supported by grants from JDRF (grant no. 3-SRA-2015-117-Q-R) and grants from the start-up packages of UCLA. We acknowledge the use of the Analytical Instrumentation Facility (AIF) at NC State, which is supported by the State of North Carolina and the NSF. A.K. is supported by the National Institute of Diabetes and Digestive and Kidney Disease of the NIH under award number F30DK113728. **Author contributions:** J.W., J.Y., J.B.B., and Z.G. designed the experiments. J.W., J.Y., Y.Z., X.Z., G.C., Z.W., W.S., Z.C., and C.Q. performed experiments. J.W., J.Y., A.R.K., L.C., Q.S., A.K., J.B.B., and Z.G. analyzed the data and wrote the paper. **Competing interests:** Z.G. and J.W. are authors on a Patent Cooperation Treaty (PCT) application for "Charge-switchable polymeric depot for glucose-triggered insulin delivery with ultrafast response" (NCSU reference no. 17275) that was filed with North Carolina State University (application no. PCT/US2018/061953, filed on 20 November 2018). J.B.'s contracted consulting fees are paid to the University of North Carolina by Adocia, AstraZeneca, Dance Biopharm, Dexcom, Elcelyx Therapeutics, Eli Lilly and Company, Fractyl, GI Dynamics, Intarcia Therapeutics, Lexicon, MannKind, Metavention, NovaTarg, Novo Nordisk, Orexigen Therapeutics, PhaseBio, Sanofi, Senseonics, Shenzhen HighTide, Takeda, vTv Therapeutics, and Zafgen. He reports grant support from AstraZeneca, Eli Lilly, GI Dynamics, GlaxoSmithKline, Intarcia Therapeutics, Johnson & Johnson, Lexicon, Medtronic, Novo Nordisk, Orexigen, Sanofi, Scion NeuroStim, Takeda, Theracos, and vTv Therapeutics. He is a consultant to Cirius Therapeutics Inc., CSL Behring, Neurimmune AG, and Whole Biome and holds stock options in Mellitus Health, PhaseBio, and Stability Health. All authors declare no other competing interests. **Data and materials availability:** All data needed to evaluate the conclusions in the paper are present in the paper and/or the Supplementary Materials. Additional data related to this paper may be requested from the authors.

Submitted 19 December 2018
Accepted 6 June 2019
Published 10 July 2019
10.1126/sciadv.aaw4357

Citation: J. Wang, J. Yu, Y. Zhang, X. Zhang, A. R. Kahkoska, G. Chen, Z. Wang, W. Sun, L. Cai, Z. Chen, C. Qian, Q. Shen, A. Khademhosseini, J. B. Buse, Z. Gu, Charge-switchable polymeric complex for glucose-responsive insulin delivery in mice and pigs. *Sci. Adv.* **5**, eaaw4357 (2019).